Clim. Past Discuss., 9, 3371–3398, 2013
www.clim-past-discuss.net/9/3371/2013/
doi:10.5194/cpd-9-3371-2013

Climate of the Past
Discussions
Open Access

Statistical downscaling of a climate simulation of the last glacial cycle: temperature and precipitation over Northern Europe

N. Korhonen[1,3], A. Venäläinen[1], H. Seppä[2], and H. Järvinen[3]

[1]Finnish Meteorological Institute, Climate Change Research Unit, Helsinki, Finland
[2]University of Helsinki, Department of Geosciences and Geography, Helsinki, Finland
[3]University of Helsinki, Department of Physics, Helsinki, Finland

Received: 27 May 2013 – Accepted: 3 June 2013 – Published: 21 June 2013

Correspondence to: N. Korhonen (natalia.korhonen@fmi.fi)

Published by Copernicus Publications on behalf of the European Geosciences Union.

CPD
9, 3371–3398, 2013

Temperature and precipitation over Northern Europe

N. Korhonen et al.

Abstract

Earth System Models of Intermediate Complexity (EMICs) have proven to be able to simulate the large-scale features of glacial-interglacial climate evolution. For many climatic applications the spatial resolution of the EMICs' output is, however, too coarse, and downscaling methods are needed. We used Generalized Additive Models (GAMs) for downscaling the large-scale output of an EMIC. GAMs are regression models in which a combination of explanatory variables are related to the response through a sum of spline functions. We calibrated the GAMs using observations of the recent past climate and the results of short time-slice simulations of glacial climate performed by the relatively high-resolution general circulation model CCSM and the regional climate model RCA3. As explanatory variables we used the output of a simulation by CLIMBER-2 EMIC of the last glacial cycle, coupled with the SICOPOLIS ice sheet model, i.e., the large-scale temperature and precipitation data of CLIMBER-2, and the elevation, distance to ice sheet, slope direction and slope angle from SICOPOLIS. The fitted GAMs were able to explain more than 96 % of the temperature response with a correlation of >0.98 and more than 59 % of the precipitation response with a correlation of >0.72. The first comparison with two pollen-based reconstructions of temperature for Northern Europe showed that CLIMBER-2 data downscaled by GAMs corresponded better with the reconstructions than did the bi-linearly interpolated CLIMBER-2 surface temperature.

1 Introduction

Climate risk assessments and bioclimatic studies on a millennial time-scale require regional climate data. Present state-of-the-art comprehensive atmospheric General Circulation Models (GCMs), coupled with modules simulating the biosphere and sea ice, are major tools for the study of past, present and future climates. The resolution of such global models is usually 100–300 km (Randall et al., 2007). The relatively high

CPD
9, 3371–3398, 2013

resolution and complex calculations make GCMs suitable for modelling the climate on a 100–1000 yr time-scale. For simulating full glacial cycles, the GCMs are computationally far too demanding. Nevertheless, several GCMs have been used for time-slice simulations of the distant past climate with prescribed ice sheets (Otto-Bliesner et al., 2006; Kjellström et al., 2010; Singarayer and Valdes, 2010; Strandberg et al., 2011; Renssen et al., 2005; Liu et al., 2009).

The models suitable for simulating glacial cycles (time-scale 100 000 yr), are Earth system models of intermediate complexity (EMICs; Claussen et al., 2002; Petoukhov et al., 2005). In terms of complexity these models lie between simple energy-balance models (e.g., Pollard, 1982) and comprehensive GCMs. EMICs have a rather low spatial resolution, enabling very long simulations with a reasonable computing time. These models include simplified component models for the atmosphere, ocean, sea ice, land surface, terrestrial vegetation, and ice sheets. These interact under the prescribed solar forcing (insolation) and atmospheric chemical composition. In an intercomparison of eight EMICs by Petoukhov et al. (2005), the EMICs' equilibrium and transient responses to a doubling of the atmospheric CO_2 concentration were within the range of corresponding GCM simulations. EMICs have been utilized in simulating past glaciations (Calov et al., 2005a, b; Wang and Mysak, 2002; Berger et al., 1999) and future climate on a time-scale of 100 000 yr (Archer and Ganopolski, 2005; Berger et al., 2003; Berger and Loutre, 2002; Cochelin et al., 2006).

The EMIC simulations provide continuous global data; however, there are uncertainties related to the model simplifications and low spatial resolution, and these make the direct output of EMICs unsuitable for regional studies. In climate science, several downscaling methods have been used. A common method is to downscale the results of a global model dynamically with a regional model. Regional models usually have sophisticated atmosphere and biosphere modules at a resolution of ∼ 50 km and are therefore computationally demanding. Hence downscaling of this kind is possible only for short time-slice simulations of 50–100 yr, not for an entire 100 000 yr-long simulation. A computationally less demanding method is statistical downscaling. In this, the

CPD
9, 3371–3398, 2013

statistical relationships between the observed small-scale variables (derived from observations) and larger-scale variables (e.g., from a global model) are derived using, for example, regression analysis. These derived statistical relations are then applied to downscale the large-scale variables of climate simulations to a smaller scale.

Vrac et al. (2007) introduced a statistical downscaling method for paleoclimatological purposes, based on Generalized Additive Models (GAMs; Wood, 2006). They fitted a GAM-type regression model by finding the statistical relationships between the observed recent past climate (1961–1990) and the low-resolution CLIMBER-2 EMIC model simulation of recent past climate. They then used this regression model to downscale the recent past and last glacial maximum climates simulated by CLIMBER-2 over Western Europe. Martin et al. (2013a, b, c) developed these GAMs further, using them to downscale the future climate 100 yr AP. All these GAMs were calibrated with the recent past climate, and were used relying on the assumption that the statistical relations between the large and small scales remain unchanged for the last glacial maximum and the future climate.

We investigated the usability of GAMs in downscaling the large-scale variables of the CLIMBER-2 EMIC model simulations by Ganopolski et al. (2010) over Europe in climatic conditions ranging from glacial to interglacial. For this purpose we fit a GAM not only to downscale the observed recent past climate but also to downscale relatively high-resolution simulated glacial climate. For a glacial period characterized by an extensive ice sheet over Fennoscandia, about 21 kyr Before Present (BP), we utilized data from a CCSM4 GCM simulation by Brady et al. (2013) and an RCA3 regional model simulation by Strandberg et al. (2011). For a glacial period characterized by a small ice sheet over Fennoscandia, about 44 kyr BP, we utilized data from an RCA3 simulation by Kjellström et al. (2010). As stated by Vrac et al. (2007), the use of statistical downscaling in palaeoclimatology is based on the assumption that the fitted regression model remains unchanged over time. We evaluated the GAMs by presenting their skill scores and investigate thereby which explanatory variables produce the best fit. We also tested the GAMs for downscaling the temperature of the CLIMBER-2

CPD
9, 3371–3398, 2013

simulation from 10 kyr BP up to the present. The bi-linearly interpolated CLIMBER-2 surface temperature and the downscaled temperature were compared to two temperature reconstructions: Laihalampi, Finland (Heikkilä and Seppä, 2003) and Gilltjärnen, Sweden (Antonsson et al., 2006).

2 Downscaling with generalized additive models

Statistical regression models are calibrated by establishing statistical relationships between large-scale variables (called explanatory variables or *predictors*, $X_1 \ldots X_p$) and a local variable (Y, called the response or *predictand*). Our large-scale data are CLIMBER-2 global model's output (Ganopolski et al., 2010) covering the last glacial cycle, with climate conditions ranging from glacial to interglacial. The range of the large-scale variables, X, defines the calibration range. Hence, the calibration range of the regression model should cover glacial to interglacial climates. For local data representing interglacial climate we utilize observations of the recent past climate by the Climate Research Unit, CRU. For local data representing climate for certain time steps of the last glacial cycle we utilize simulations by a GCM (CCSM4, Gent et al., 2011) and a regional model (RCA3, Samuelsson et al., 2011). We aim at finding the relationships between the high-resolution data and the large-scale data for the corresponding time periods. These relationships are then used with the large-scale data to obtain high-resolution data where they are otherwise not available.

2.1 Calibrating the statistical model

We used GAMs (Hastie and Tibshirani, 1990; Wood, 2006) in which the statistical expectation (E) of the predictand (Y) was modelled using the sum of univariate spline

CPD
9, 3371–3398, 2013

functions of the p predictors $(X_1\ldots,X_p)$, such that

$$E(Y|X_1\ldots X_p) = \sum_{j=1}^{p} f_j(X_j) + \varepsilon \tag{1}$$

where the potentially non-linear spline functions f_j had a non-parametric form. The residuals, ε, were expected to be normally distributed. The calibration of GAMs is data-driven, and the shape of the response is not forced to any parametric form. GAMs are called semiparametric models, as the probability distribution of the predictand should be known. Our predictand was either the mean temperature or the mean total precipitation. As temperature data classically satisfy the normality assumption, the response variable mean temperature was expected to follow a normal distribution. According to Cheng and Qi (2002), the cumulative precipitation data can be modelled by a log-normal distribution, hence the total precipitation response variable was log-transformed and expected to follow a normal distribution. The statistical relationships were calibrated by stepwise screening of the data, using the data for one month (or annual) at a time. For fitting the GAM, all the data were to be represented at the same spatial resolution. We used a resolution of 1.5° × 0.75° over Northern Europe (54° N… 70° N and 3° E… 35° E) and Western Eurasia (36° N… 70° N and 10° W… 69° E). As the sizes of the grid cells of our data varied with latitude, we associated a weight to each grid cell depending on the latitude of the data. The functions f_j in Eq. (1) were defined by cubic regression splines with a restricted maximum number of degrees of freedom under wiggliness penalization (Wood, 2006). This means that although the maximum number of the degrees of freedom per predictor was restricted here to 15, the penalization allowed reducing the effective number of degrees of freedom of each spline to what was really needed by the problem.

As predictors on the right-hand side of Eq. (1) we used both meteorological and geographic predictors. As meteorological predictors we tested CLIMBER-2 large-scale temperature, relative humidity, precipitation, and lapse rate data. As geographic predictors we tested terrain properties (elevation, shortest distance to the ocean, distance to nearest water body, slope angle, direction of the slope with respect to the north), latitude, longitude, and shortest distance to the ice sheet margin. The predictor side's temperature, relative humidity, precipitation, lapse rate and, over ice free areas, the terrain properties were extracted from the CLIMBER-2-SICOPOLIS simulation data by Ganopolski et al. (2010) at 0 kyr BP, 44 kyr BP and 21 kyr BP to represent the recent past, a stadial during MIS 3 and LGM, respectively. Over ice-covered areas the terrain properties used as predictors were extracted from the data of the RCA3 and CCSM4 simulations. The shortest distance to the nearest glacier margin used as predictor was computed from the RCA3 and CCSM4 ice sheet data. In ice-free areas the distance was expressed by positive values and on areas covered by ice the distance was expressed by negative values.

The final predictors were determined by minimization of the Generalized Cross-Validation (GCV) score, which was computed by:

$$\mathrm{GCV} = \frac{\overline{N(Y_\mathrm{m} - \overline{Y_\mathrm{m}})^2}}{(N - \gamma d)^2} \tag{2}$$

where N stands for the number of observations Y_m for the GAM-modelled surface air temperature or log-precipitation, and d stands for the effective number of degrees of freedom. The GCV score is an estimate of the expected mean square predictor error inside the calibration predictor values' range. The GCV has the same units as Y. Further, in computing the GCV, the effective degrees of freedom were also penalized by increasing their cost with a weight $\gamma = 1.4$ to prevent over-fitting of the model. We allowed ourselves to combine several predictors, if that was found to improve the skill scores and was physically reasonable. We tested numerous combinations of predictors for fitting the GAMs in Eq. (1). Based on the GCV values, the best fits for downscaling the log-precipitation with GAMs were yielded by:

$$\log(P)(P_\mathrm{CLI}, x, y, h, d) = s_1(P_\mathrm{CLI}) + s_2(x, y) + s_3(h) + s_4(d), \tag{3}$$

CPD
9, 3371–3398, 2013

in which P represents the downscaled precipitation, P_{CLI} is the precipitation of the large-scale data (CLIMBER-2), x and y are the longitude and latitude, respectively, h is the elevation, d is the direction of the steepest slope, and $s_1 \ldots s_4$ are spline functions.

For downscaling the annual temperature and the monthly temperature of May, June, July, August and September with GAMs, the best fits were yielded by:

$$T(T_{\mathrm{CLI}}, x, y, h, i) = T_{\mathrm{CLI}} + s_5(x, y) + s_6(h, i), \tag{4}$$

and for the monthly temperature of January, February, March, April, October, November and December by:

$$T(T_{\mathrm{CLI}}, x, y, h, d, s) = T_{\mathrm{CLI}} + s_7(x, y, T_{\mathrm{CLI}}) + s_8(h) + s_9(d, s) \tag{5}$$

in which T is the downscaled temperature, T_{CLI} is the temperature of the large-scale data (CLIMBER-2), the slope, s, is the angle of the steepest slope, i is the shortest distance to the ice sheet margin (positive if ice free, negative if covered with ice) and $s_5 \ldots s_9$ are spline functions.

2.2 Large-scale input data, CLIMBER-2-SICOPOLIS

The large-scale data to be downscaled were the output of a full last glacial cycle simulation (126 000 yr BP until the present-day) with the CLIMBER-2-SICOPOLIS model system by Ganopolski et al. (2010). CLIMBER-2 is an EMIC consisting of six Earth system components: atmosphere, ocean, sea ice, land surface, terrestrial vegetation and ice sheets (Petoukhov et al., 2000). The model has a relatively low spatial resolution: for the atmospheric module the latitudinal resolution is 10° and the longitudinal resolution is roughly 51°. The CLIMBER-2 model successfully describes the seasonal variability of a large set of characteristics of the climate system (Petoukhov et al., 2000), and simulates the climate response to changes in different types of forcing and boundary conditions within the range of corresponding GCM simulations (Ganopolski et al., 2001; Petoukhov et al., 2005). For simulating glacial climates, the CLIMBER-2 model has been coupled with the high resolution 3-dimensional thermomechanical

CPD
9, 3371–3398, 2013

ice sheet model SICOPOLIS (Greve, 1997). The resolution of the ice sheet model is $1.5^\circ \times 0.75^\circ$ and the model domain extends in the Northern Hemisphere from 21° N to 85.5° N. The climate and ice sheet components are coupled bi-directionally using a physically-based energy and mass balance interface (SEMI) as described in detail by Calov et al. (2005a). The simulations by Ganopolski et al. (2010) were forced by variations in the Earth's orbital parameters calculated following Berger (1978), and atmospheric greenhouse gas concentrations derived from the Vostok ice core. The evolution of the radiative forcing of atmospheric dust was parameterized to alter proportionally with the simulated global ice volume as by Schneider et al. (2006).

2.3 Regional-scale input data

2.3.1 Recent past climate

For the recent past climate predictands, we used the Climate Research Unit (CRU) high-resolution climate data, version 2.1. (Mitchell and Jones, 2005). For land areas the original resolution of the monthly mean surface temperature and total precipitation data was $0.5^\circ \times 0.5^\circ$. To cover areas where CRU high-resolution data were not available, i.e., sea areas, we used the Jones et al. (1999) $5^\circ \times 5^\circ$ temperature data. Similarly, where high-resolution precipitation data were not available, we used the Climate Prediction Center (CPC) Merged Analysis of Precipitation (CMAP, Xie and Arkin, 1997) derived from the years 1979 to 2000, with the original data resolution of $2.5^\circ \times 2.5^\circ$.

2.3.2 Glacial climate over Northern Europe

For the glacial climate predictands over Northern Europe (54° N . . . 70° N and 3° E . . . 35° E) we used the monthly mean temperature and precipitation values of two simulations with the regional climate model RCA3 (Kjellström et al., 2005; Samuelsson et al., 2011) forced by simulations with the GCM CCSM3 (Collins et al., 2006; Kiehl et al., 2006; Otto-Bliesner et al., 2006). The first data set was that of an RCA3

Discussion Paper | Discussion Paper | Discussion Paper | Discussion Paper |

CPD

9, 3371–3398, 2013

Temperature and precipitation over Northern Europe

N. Korhonen et al.

Title Page
Abstract Introduction
Conclusions References
Tables Figures
◀| |▶
◀ ▶
Back Close
Full Screen / Esc

Printer-friendly Version

Interactive Discussion

simulation by Kjellström et al. (2010), representing a stadial within the Marine Isotope Stage 3 (MIS 3) around 44 000 yr BP, a cold period with a relatively small Fennoscandian ice sheet as illustrated in Fig. 1a. The second data set was that of an RCA3 simulation by Strandberg et al. (2011), representing the Last Glacial Maximum (LGM) around 21 000 yr BP, with an extensive ice sheet covering large parts of North Eurasia, as illustrated in Fig. 1b.

2.3.3 Glacial climate over Western Eurasia

The glacial climate predictands over Western Eurasia (36° N ... 70° N and 10° W ... 69° E) were produced using annual mean temperature and precipitation data from two simulations with GCM CCSM4: the last 20 yr of the CCSM4 LGM simulation (Brady et al., 2013) and the period 1961–1990 AD of the CCSM4 historical simulation (Gent et al., 2011). First we computed the differences between the CCSM4 simulated LGM and historical climates and then we added these changes to the CRU's annual temperature and precipitation data sets (Sect. 2.3.1). For temperature we applied the absolute change (°C) and for precipitation the relative change (%).

2.4 Evaluation of the GAMs

For evaluating the fitted GAMs, we computed several statistical quantities, as follows:

(i) the percentage of Explained Deviance

$$\%\mathrm{ED} = 100 \times \frac{\overline{\left(Y_\mathrm{m} - \overline{Y_0}\right)^2}}{\overline{\left(Y_0 - \overline{Y_0}\right)^2}}, \tag{6}$$

where Y_0 stands for the predictand data (CRU/RCA3/CCSM4) and Y_m for the GAM-modelled surface air temperature or log-precipitation;

CPD
9, 3371–3398, 2013

(ii) the spatial correlation between the CRU/RCA3/CCSM4 and the GAM-modelled surface air temperature or log-precipitation

$$\mathrm{Cor} = \frac{\langle (Y_\mathrm{m} - \langle Y_\mathrm{m} \rangle) \cdot (Y_0 - \langle Y_0 \rangle) \rangle}{\sqrt{\langle (Y_\mathrm{m} - \langle Y_\mathrm{m} \rangle)^2 \rangle \cdot \langle (Y_0 - \langle Y_0 \rangle)^2 \rangle}}, \tag{7}$$

and (iii) the explained variance:

$$\mathrm{ev} = \frac{\langle (Y_\mathrm{m} - \langle Y_0 \rangle)^2 \rangle}{\langle (Y_0 - \langle Y_0 \rangle)^2 \rangle}. \tag{8}$$

For error estimates we computed the root-mean-square error

$$\mathrm{RMSE} = \sqrt{n^{-1} \sum_{i=1}^{n} (Y_0 - Y_\mathrm{m})^2}, \tag{9}$$

which is sensitive to the maximum errors, and the mean absolute difference

$$\mathrm{MAD} = n^{-1} \sum_{i=1}^{n} |Y_0 - Y_\mathrm{m}|, \tag{10}$$

which is less sensitive to the maximum errors.

2.5 Comparison with temperature reconstructions

The calibrated GAMs were applied to downscale the Holocene climate (10 kyr BP until the present) of the simulation by Ganopolski et al. (2010). The produced annual mean temperature was compared with two pollen-based reconstructions of temperature for Laihalampi, Finland (Heikkilä and Seppä, 2003) and Gilltjärnen, Sweden (Antonsson et al., 2006). The RMSE and MAD were computed for the bi-linearly interpolated CLIMBER-2 surface temperature and the reconstructions as well as for the downscaled temperature and the reconstructions.

CPD
9, 3371–3398, 2013

3 Results

Equation (3) resulted in the skill scores presented in Table 1. The precipitation GAMs showed good correlation (> 0.72) with the fitted data. The MAD (RMSE) of the monthly precipitation GAMs varied between 7 mm month^{-1} (12 mm month^{-1}) in February and 12 mm month^{-1} (21 mm month^{-1}) in October. The GAMs were able to explain the spatial variance of the total precipitation by 59 to 85 %.

Figure 2 depicts the splines of the GAM downscaling January log-precipitation over Northern Europe. Figure 2a demonstrates the effect of the raw CLIMBER-2 January precipitation: the precipitation increased with CLIMBER-2's precipitation, indicating that CLIMBER-2 output was generally well consistent with the high-resolution data. Figure 2b shows the effect of the longitude and latitude: the spline increased precipitation on the west coast of Norway, as well as in Denmark and Southern Sweden and decreased it over Central and Northern Finland. The effect of elevation on precipitation depended on the season. In the annual GAM and March to September GAMs, the precipitation increased with elevation (not shown). On the other hand, for cooler months, October to January, the elevation effect was weaker, and for elevations between 1000 and 2000 m the precipitation even decreased with elevation (Fig. 2c). The effect of the direction of the slope is shown in Fig. 2d: southerly and westerly slopes ($\sim 180^{\circ}$ to $\sim 270^{\circ}$) tended to increase precipitation, whereas northerly and easterly slopes ($\sim 0^{\circ}$ to $\sim 90^{\circ}$) decreased it.

Figure 3 demonstrates the raw CLIMBER-2 January precipitation (top row in Fig. 3), the CRU (first figure of the second row in Fig. 3) and RCA3 (second and third figures of the second row in Fig. 3) regional scale precipitation, the GAM downscaled January precipitation (third row in Fig. 3), and the difference between the CRU/RCA3 data and the GAM downscaled precipitation (bottom row in Fig. 3). By comparing rows three and two in Fig. 3, we see that the GAM reproduced well the spatial distribution of precipitation over Northern Europe, the highest precipitation rates occurring on the western slopes of the Scandinavian mountains and the smallest over the central parts of the Fennoscandian ice sheet.

Equations (4) and (5) resulted in the skill scores presented in Table 2. For the temperature GAMs the correlations were high, explaining 96 to 99 % of the spatial variance of mean temperature. The MAD (RMSE) of the temperature GAMs varied between 0.6 °C (0.8 °C) in April and 1.6 °C (2.2 °C) in January. The calibration ranges of the monthly and annual mean temperatures over the inspection area (Northern Europe or Western Eurasia) are also shown in Table 2. The calibration ranged from a glacial to an interglacial climate. The CLIMBER-2 temperature was used directly, i.e., linearly, see Eqs. (4) and (5). With the splines for longitude and latitude some of the cold bias of CLIMBER-2 over Northern European land areas was corrected, as seen for the July temperature GAM in Fig. 4a. Over Western Eurasia, the longitude and latitude splines produced warming over Western Europe and cooling over continental Russia (not shown). In all the GAMs, the splines decreased the temperature with increasing altitude, as shown for July in Fig. 4b. In the May–September and annual GAMs (Eq. 4) the splines also decreased the temperature with increasing distance to ice-free areas, as shown for July in Fig. 4b. In the GAMs for October–April (Eq. 5) the direction of the slope also seemed to have an influence on the local temperature: the splines increased the temperature on the westerly slopes and decreased it on the easterly slopes (not shown).

In Fig. 5 the bi-linearly interpolated CLIMBER-2 July temperatures are in the top row, the CRU observed July temperature is in the first figure of the second row, the RCA3 simulated July temperatures are in the second and third figures of the second row, the GAM downscaled July temperatures are in the third row, and the differences between the CRU/RCA3 data and the GAM downscaled temperatures are in the bottom row. By comparing rows three and two in Fig. 5, we see that the GAM reproduced well the spatial distribution of July temperature over Northern Europe, e.g., the Scandinavian mountains and the strong temperature gradient near the ice sheet margin were well brought out by the GAM. The GAM seemed to work especially well on ice-free land

CPD
9, 3371–3398, 2013

areas that were not in the close vicinity of ice sheets or mountains, the residuals being typically 0–2 °C. There were, however, also some differences, e.g., the downscaling of the recent past climate over the Scandinavian mountains was somewhat too cold, and the temperature gradient on the eastern margin of the ice sheet in the downscaled GAMs was less steep than in the RCA3 simulation.

Figure 6 shows pollen-based reconstructions of annual mean temperature, the bi-linear interpolation of the annual mean surface temperature simulated by CLIMBER-2, and the GAM downscaled annual mean temperature at two locations in Northern Europe during the Holocene. The pollen-based reconstructions were produced with a weighted averaging-partial least square regression and calibration technique and include a general error of 1.0–1.5 °C (Birks et al., 2010). When proxy-based reconstructions are used for comparison with model results, it must be borne in mind that the output of such reconstructions have been shown to be sensitive to the spatial extents of the used calibration data-sets (Salonen et al., 2013). However, while the absolute values are highly sensitive to the climatic characteristics of the calibration dataset, the shapes of the relative palaeotemperature curves seem comparatively robust, as the curve shapes mostly remain similar as the calibration data is spatially shifted (Salonen et al., 2013). Hence it is important to note that the shapes of the reconstructed temperature curves are generally consistent with those based on GAM downscaling for the Holocene (Fig. 6). As for the absolute values, the MAD of the reconstructions and the bi-linear interpolation of the CLIMBER-2 surface temperature was larger than 3.8 °C and the RMSE > 3.9 °C. The MAD of the reconstructions of the GAM output was less than 1.4 °C and the RMSE < 1.6 °C.

4 Discussion and conclusions

We found that with an apt selection of predictor parameters, Generalized Additive Models (GAMs) can be useful to statistically downscale low-resolution CLIMBER-2 EMIC simulation data ranging from a glacial to an interglacial climate. For calibrating the

CPD
9, 3371–3398, 2013

GAMs, we utilized both physical predictors – such as the large-scale precipitation and temperature data of CLIMBER-2 – and geographical predictors – such as elevation, latitude, longitude, the direction of the steepest slope, the angle of the steepest slope, and the shortest distance to the ice sheet margin. The final selection of predictors was based on the statistical skill scores of each GAM.

The GAMs fitted for temperature (precipitation) were able to approximately reproduce the observed and modelled temperature (precipitation) fields. The mean errors in the mean temperature (total precipitation) were of an order of magnitude of 1 to 2 °C (10–20 mm month^{-1}) as the climate varied from glacial to interglacial over Europe. These error estimates are larger than in the GAMs by Martin et al. (2013a, b); however, so too is the calibration range of our GAMs: the calibration ranges in Martin et al. (2013a, b) covered only an interglacial climate, whereas our fitting included a glacial climate as well.

One critical assumption in the use of statistical downscaling method is that the statistical relationship of the used climate parameters should remain stationary over time (Vrac et al., 2007). This assumption can be questioned with palaeoclimatic simulations spanning tens of thousands of years and reaching back to the last glacial with markedly different climatic boundary values than at present. For the validation of the statistical downscaling method, we compared our simulated Holocene temperatures with two pollen-based quantitative annual mean temperature reconstructions from Finland and Sweden. The results of these comparisons were generally congruent and thus support the validity of the statistical downscaling approach at least in Northern Europe. Moreover, GAM downscaled CLIMBER-2 temperature showed better agreement with the pollen-based reconstructions than the bi-linearly interpolated CLIMBER-2 surface temperature.

The downscaling method enables the generation of high-resolution climate data from the low resolution CLIMBER-2-SICOPOLIS simulations of the past and future. These data could be used in bioclimatic modelling and long-term climate assessment. The first comparison of the GAM downscaled CLIMBER-2 temperature to paleoclimatological reconstructions showed better agreement than did the bi-linearly interpolated CLIMBER-2 temperature. To further study the correspondence of these downscaled simulations, the next step will be to downscale the precipitation and temperature with the fitted GAMs over the whole last glacial cycle simulation, and compare the results with paleoclimatological reconstructions. Finally, the GAMs could be further developed by adding predictors or additional simulation data such as the ensemble mean of the PMIP3 LGM simulations.

Acknowledgements. We are grateful to Andrey Ganopolski from the Potsdam Institute for Climate Impact Research for providing the climate simulations of CLIMBER-2-SICOPOLIS, to Gustav Strandberg and Erik Kjellström from the Swedish Meteorological and Hydrological Institute for the regional climate simulations with the RCA3 model, the Climate Research Unit for the 1961–1990 high-resolution temperature and precipitation data, to NOAA/OAR/ESRL PSD, Boulder, USA for the CMAP Precipitation data, and to the contributors to the R project. The GAM fitting was done using the R software package "mgcv" downloaded from the website of the R project for statistical computing (http://www.r-project.org/). We acknowledge all those involved in producing the PMIP and CMIP multi-model ensembles and data syntheses, and the World Climate Research Programme's Working Group on Coupled Modelling, which is responsible for CMIP, and the climate modelling group at NCAR, Boulder, USA, for producing and making available their CCSM4 model output. For CMIP the US Department of Energy's Program for Climate Model Diagnosis and Intercomparison provides coordinating support, and led the development of software infrastructure in partnership with the Global Organization for Earth System Science Portals. We acknowledge Posiva PLC for funding the writing of this paper. This publication is contribution number 24 of the Nordic Centre of Excellence SVALI, "Stability and Variations of Arctic Land Ice", funded by the "Nordic Top-level Research Initiative (TRI)". The research has been partly funded by the Academy of Finland (project number 140771).

References

Antonsson, K., Brooks, S. J., Seppä, H., Telford, R. J., and Birks, H. J. B.: Quantitative palaeotemperature records inferred from fossil pollen and chironomid assemblages from Lake Gilltjärnen, northern central Sweden, J. Quaternary Sci., 21, 831–841, 2006.

Archer, D. and Ganopolski, A.: A movable trigger: fossil fuel CO_2 and the onset of the next glaciation, Geochem. Geophy. Geosy., 6, Q05003, doi:10.1029/2004GC000891, 2005.
Berger, A.: Long-term variations of caloric insolation resulting from the Earth's orbital elements, Quarternary Res., 9, 139–167, 1978.
Berger, A. and Loutre, M. F.: An exceptionally long interglacial ahead?, Science, 297, 1287–1288, 2002.
Berger, A., Li, X. S., and Loutre, M. F.: Modeling Northern Hemisphere ice volume over the last 3 million years, Quaternary Sci. Rev., 18, 1–11, 1999.
Berger, A., Loutre, M. F., and Crucifix, M.: The Earth's climate in the next hundred thousand years (100 kyr), Surv. Geophys., 24, 117–138, 2003.
Birks, H. J. B., Heiri, O., Seppä, H., and Bjune, A. E.: Strengths and weaknesses of quantitative climate reconstructions based on Late-Quaternary biological proxies, Open Ecology Journal, 3, 68–110, 2010.
Brady, E., Otto-Bliesner, B., Kay, J., and Rosenbloom, N.: Sensitivity to glacial forcing in the CCSM4, J. Climate, 26, 1901–1925, doi:10.1175/JCLI-D-11-00416.1, 2013.
Calov, R., Ganopolski, A., Claussen, M., Petoukhov, V., and Greve, R.: Transient simulation of the last glacial inception, Part I: glacial inception as a bifurcation in the climate system, Clim. Dynam., 24, 545–561, 2005a.
Calov, R., Ganopolski, A., Claussen, M., Petoukhov, V., Claussen, M., Brovkin, V., and Greve, R.: Transient simulation of the last glacial inception, Part II: sensitivity and feedback analysis, Clim. Dynam., 24, 563–576, 2005b.
Cheng, M. and Qi, Y.: Frontal rainfall rate distribution and some conclusions on the threshold method, J. App. Meteorol., 41, 1128–1139, 2002.
Claussen, M., Mysak, L., Weaver, A., Crucifix, M., Fichefet, T., Loutre, M. F., Weber, S., Alcamo, J., Alexeev, V., Berger, A., Calov, R., Ganopolski, A., Goosse, H., Lohmann, G., Lunkeit, F., Mokhov, I., Petoukhov, V., Stone, P., and Wang, Z.: Earth system models of intermediate complexity: closing the gap in the spectrum of climate system models, Clim. Dynam., 18, 579–586, 2002.
Cochelin, A.-S. B., Mysak, L. A., and Wang, Z.: Simulation of long-term future climate changes with the green McGill paleoclimate model: the next glacial inception, Climatic Change, 79, 381–401, 2006.
Collins, W. D., Bitz, C. M., Blackmon, M. L., Bonan, G. B., Bretherton, C. S., Carton, J. A., Chang, P., Doney, S. C., Hack, J. J., Henderson, T. B., Kiehl, J. T., Large, W. G.,

CPD
9, 3371–3398, 2013

Temperature and precipitation over Northern Europe

N. Korhonen et al.

McKenna, D. S., Santer, B. D., and Smith, R. D.: The Community Climate System Model Version 3 (CCSM3), J. Climate, 19, 2122–2143, 2006.
Ganopolski, A., Petoukhov, V., Rahmstorf, S., Brovkin, V., Claussen, M., Eliseev, A., and Kubatzki, C.: CLIMBER-2: a climate system model of intermediate complexity, Part II: model sensitivity, Clim. Dynam., 17, 735–751, 2001.
Ganopolski, A., Calov, R., and Claussen, M.: Simulation of the last glacial cycle with a coupled climate ice-sheet model of intermediate complexity, Clim. Past, 6, 229–244, doi:10.5194/cp-6-229-2010, 2010.
Gent, P. R., Danabasoglu, G., Donner, L. J., Holland, M. M., Hunke, E. C., Jayne, S. R., Lawrence, D. M., Neale, R. B., Rasch, P. J., Vertenstein, M., Worley, P. H., Yang, Z.-L., and Zhang, M.: The Community Climate System Model Version 4, J. Climate, 24, 4973–4991, 2011.
Greve, R.: Application of a polythermal three-dimensional ice sheet model to the Greenland ice sheet: response to steady-state and transient climate scenarios, J. Climate, 10, 901–918, 1997.
Hastie, T. and Tibshirani, R.: Generalized Additive Models, monographs on statistics and applied probability, Vol. 43, Chapman & Hall, New York, 1990.
Heikkilä, M. and Seppä, H.: A 11 000 yr palaeotemperature reconstruction from the southern boreal zone in Finland, Quaternary Sci. Rev., 22, 541–554, 2003.
Jones, P. D., New, M., Parker, D. E., Martin, S., and Rigor, I. G.: Surface air temperature and its changes over the past 150 yr, Rev. Geophys., 37, 173–199, 1999.
Kiehl, J. T., Shields, C. A., Hack, J. J., and Collins, W. D.: The climate sensitivity of the Community Climate System Model Version 3 (CCSM3), J. Climate, 19, 2584–2596, 2006.
Kjellström, E., Bärring, L., Gollvik, S., Hansson, U., Jones, C., Samuelsson, P., Rummukainen, M., Ullerstig, A., Willén, U., and Wyser, K.: A 140 yr simulation of European climate with the new version of the Rossby Centre regional atmospheric climate model (RCA3), Reports Meteorology and Climatology, 108, SMHI, SE-60176 Norrköping, Sweden, 54 pp., 2005.
Kjellström, E., Brandefelt, J., Näslund, J. O., Smith, B., Strandberg, G., Voelker, A. H. L., and Wohlfarth, B.: Simulated climate conditions in Fennoscandia during a MIS 3 stadial, Boreas, 39, 436–456, 2010.
Liu, Z., Otto-Bliesner, B. L., He, F., Brady, E. C., Tomas, R., Clark, P. U., Carlson, A. E., Lynch-Stieglitz, J., Curry, W., Brook, E., Erickson, D., Jacob, R., Kutzbach, J., and Cheng, J.: Tran-

sient simulation of last deglaciation with a new mechanism for Bølling–Allerød Warming, Science, 325, 310–314, 2009.
Martin, A., Vrac, M., Paillard, D., Dumas, C., and Kageyama, M.: Statistical-dynamical downscaling for an Earth Model of Intermediate Complexity, Part I: methodology and calibrations, Clim. Dynam., submitted, 2013a.
Martin, A., Vrac, M., Paillard, D., Dumas, C., and Kageyama, M.: Statistical-dynamical downscaling for an Earth Model of Intermediate Complexity, Part II: application to past and future climates, Clim. Dynam., submitted, 2013b.
Martin, A., Paillard, D., Vrac, M., Dumas, C., Kageyama, M., and Brulhet, J.: Potential climate change over the next million years: regional projections over Europe using an EMIC and a downscaling method, Climatic Change, submitted, 2013c.
Mitchell, T. D. and Jones, P. D.: An improved method of constructing a database of monthly climate observations and associated high-resolution grids, Int. J. Climatol., 25, 693–712, 2005.
Otto-Bliesner, B. L., Brady, E. C., Clauzet, G., Tomas, R., Levis, S., and Kothavala, Z.: Last glacial maximum and Holocene climate in CCSM3, J. Climate, 19, 2526–2544, 2006.
Peltier, W. R.: Global glacial isostacy and the surface of the ice-age circulation, Earth: the ICE-5G (VM2) model and GRACE, Annu. Rev. Earth Pl. Sc., 32, 111–149, 2004.
Petoukhov, V., Ganopolski, A., Brovkin, V., Claussen, M., Eliseev, A., Kubatzki, and Rahmstorf, S.: CLIMBER-2: a climate system model of intermediate complexity, Part I: model description and performance for present climate, Clim. Dynam., 16, 1–17, 2000.
Petoukhov, V., Claussen, M., Berger, A., Crucifix, M., Eby, M., Eliseev, A. V., Fichefet, T., Ganopolski, A., Goosse, H., Kamonkovich, I., Mokhov, I. I., Montoya, M., Mysak, L. A., Sokolov, A., Stone, P., Wang, Z., and Weaver, A. J.: EMIC Intercomparison Project (EMIP-CO_2): comparative analysis of EMIC simulations of climate, and of equilibrium and transient responses to atmospheric CO_2 doubling, Clim. Dynam., 25, 363–385, 2005.
Pollard, D.: A simple ice-sheet model yields realistic 100 kyr glacial cycles, Nature, 296, 334–338, 1982.
Randall, D. A., Wood, R. A., Bony, S., Colman, R., Fichefet, T., Fyfe, J., Kattsov, V., Pitman, A., Shukla, J., Srinivasan, J., Stouffer, R. J., Sumi, A., and Taylor, K. E.: Cilmate models and their evaluation, in: Climate Change 2007: The Physical Science Basis. Contribution of Working Group I to the Fourth Assessment Report of the Intergovernmental Panel on Climate Change, edited by: Solomon, S., Qin, D., Manning, M., Chen, Z., Marquis, M., Averyt, K. B.,

Tignor, M., and Miller, H. L., Cambridge University Press, Cambridge, UK and New York, NY, USA, 2007.
Renssen, H., Goosse, H., Fichefet, T., Brovkin, V., Driesschaert, E., and Wolk, F.: Simulating the Holocene climate evolution at northern high latitudes using a coupled atmosphere-sea ice-ocean-vegetation model, Clim. Dynam., 24, 23–43, 2005.
Salonen, J. S., Seppä, H., and Birks, H. J. B.: The effect of calibration data-set selection on quantitative palaeoclimate reconstructions, Holocene, submitted, 2013.
Samuelsson, P., Jones, C., Willén, U., Ullerstig, A., Gollvik, S., Hansson, U., Kjellström, E., Nikulin, G., and Wyser, K.: The Rossby Centre Regional Climate Model RCA3: model description and performance, Tellus, 63A, 4–23, 2011.
Singarayer, J. S. and Valdes, P. J.: High-latitude climate sensitivity to ice-sheet forcing over the last 120 kyr, Quaternary Sci. Rev., 29, 43–55, 2010.
Schneider von Deimling, T., Held, H., Ganopolski, A., and Rahmstorf, S.: Climate sensitivity estimated from ensemble simulations of glacial climate, Clim. Dynam., 27, 149–163, 2006.
Strandberg, G., Brandefelt, J., Kjellström, E., and Smith, B.: High resolution regional simulation of Last Glacial Maximum climate in Europe, Tellus, 63A, 107–125, 2011.
Vrac, M., Marbaix, P., Paillard, D., and Naveau, P.: Non-linear statistical downscaling of present and LGM precipitation and temperatures over Europe, Clim. Past, 3, 669–682, doi:10.5194/cp-3-669-2007, 2007.
Wang, Z. and Mysak, L.: Simulation of the last glacial inception and rapid ice sheet growth in the McGill Paleoclimate Model, Geophys. Res. Lett., 29, 2102, doi:10.1029/2002GL015120, 2002.
Wood, S. N.: Generalized Additive Models: An Introduction with R, CRC/Chapman and Hall, Boca Raton, Florida, 2006.
Xie, P. and Arkin, P. A.: Global precipitation: a 17 yr monthly analysis based on gauge observations, satellite estimates, and numerical model outputs, B. Am. Meteorol. Soc., 78, 2539–2558, 1997.

CPD
9, 3371–3398, 2013

Table 1. Skill scores of the monthly total log-precipitation GAMs for the Northern European area, and of the annual total log-precipitation (*) GAM for the Western Eurasian area. Values in parentheses represent total precipitation. The GCV score is defined in Eq. (2). The percentage of explained deviance (%ED), the spatial correlation (Cor), explained variance (ev), the root mean squared error (RMSE), and mean absolute difference (MAD) are defined in Eqs. (6)–(10), respectively.

Month	GCV	%ED (%)	Cor	ev	RMSE ($mm\,month^{-1}$)	MAD ($mm\,month^{-1}$)
Jan	0.09	84	0.91 (0.88)	0.82 (0.66)	14	8
Feb	0.09	82	0.90 (0.87)	0.80 (0.61)	12	7
Mar	0.08	79	0.89 (0.84)	0.77 (0.56)	13	7
Apr	0.08	67	0.82 (0.75)	0.66 (0.50)	13	8
May	0.06	63	0.80 (0.75)	0.61 (0.49)	13	8
Jun	0.06	63	0.80 (0.74)	0.63 (0.57)	14	10
Jul	0.06	67	0.82 (0.78)	0.67 (0.66)	15	11
Aug	0.06	59	0.77 (0.72)	0.58 (0.55)	17	12
Sep	0.07	63	0.79 (0.77)	0.60 (0.49)	20	12
Oct	0.08	72	0.85 (0.78)	0.70 (0.52)	21	12
Nov	0.10	78	0.88 (0.83)	0.75 (0.62)	18	11
Dec	0.10	81	0.90 (0.85)	0.79 (0.59)	18	10
Annual*	0.05	85	0.92 (0.84)	0.85 (0.69)	13	8

CPD
9, 3371–3398, 2013

Table 2. Skill scores and calibration ranges of the monthly mean temperature GAMs for the Northern European area, and of the annual mean temperature (*) GAM for the Western Eurasian area. Same abbreviations as in Table 1.

Month	GCV	%ED (%)	Cor	ev	RMSE (°C)	MAD (°C)	Min. Range (°C)	Max. Range (°C)
Jan	3.96	98	0.99	0.98	2.19	1.62	−37.3	−12.6
Feb	3.42	98	0.99	0.98	2.05	1.47	−36.9	−11.6
Mar	1.51	99	0.99	0.98	1.36	0.97	−32.1	−8.1
Apr	0.52	99	0.99	0.99	0.79	0.57	−23.4	−2.6
May	1.74	96	0.98	0.97	1.46	1.09	−13.9	3.8
Jun	1.96	96	0.98	0.97	1.53	1.15	−5.4	10.2
Jul	1.98	97	0.98	0.97	1.55	1.11	−0.1	13.0
Aug	2.10	96	0.98	0.97	1.58	1.19	−1.6	12.1
Sep	2.20	97	0.98	0.97	1.64	1.22	−8.5	7.7
Oct	1.63	99	0.99	0.99	1.42	1.04	−17.6	1.6
Nov	2.69	99	0.99	0.98	1.82	1.32	−26.7	−4.8
Dec	3.53	98	0.99	0.98	2.07	1.54	−33.9	−10.0
Annual*	2.2	98	0.99	0.96	1.8	1.3	−9.2	3.3

CPD
9, 3371–3398, 2013

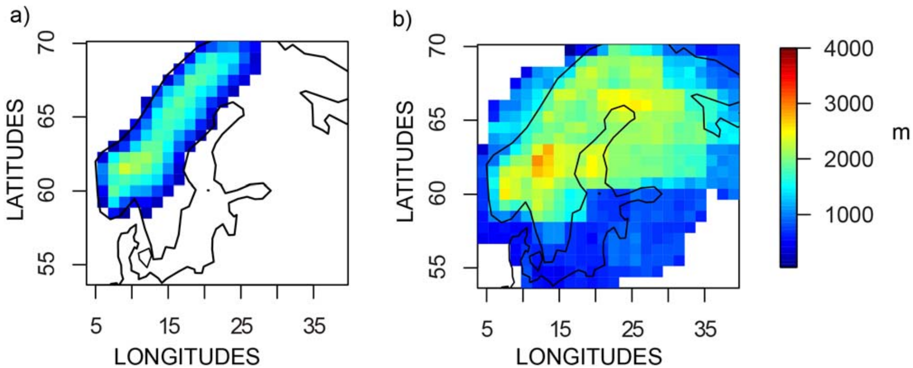

Fig. 1. Fennoscandian ice sheet extent and elevation (m) **(a)** as in the RCA3 MIS 3 stadial simulation by Kjellström et al. (2010) and **(b)** as extracted from the ICE-5G data by Peltier (2004) for the RCA3 LGM simulation by Strandberg et al. (2011).

CPD
9, 3371–3398, 2013

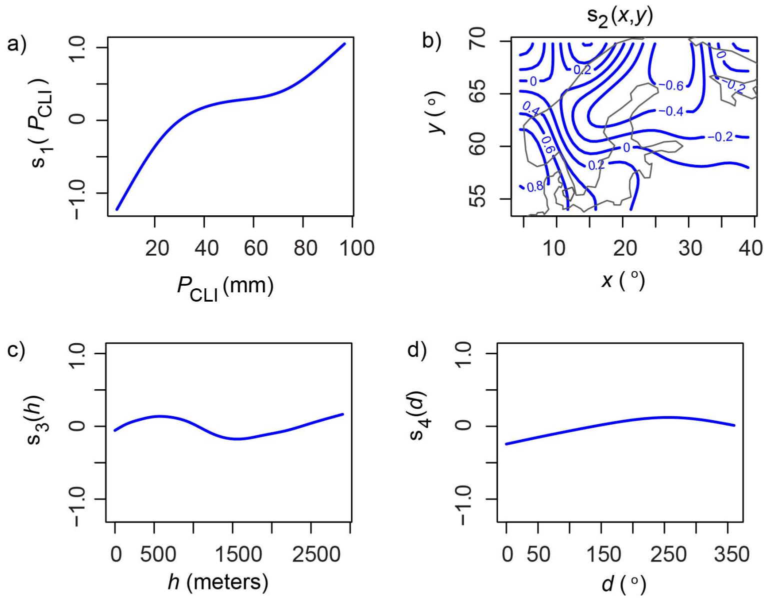

Fig. 2. Components of the GAM model in Eq. (3) fitted to downscale the CLIMBER-2 January log-precipitation in the recent past, MIS 3 stadial and LGM climates. The blue curves show the estimated effects of **(a)** CLIMBER-2 total precipitation, **(b)** longitude and latitude, **(c)** elevation, and **(d)** direction of the steepest slope.

CPD
9, 3371–3398, 2013

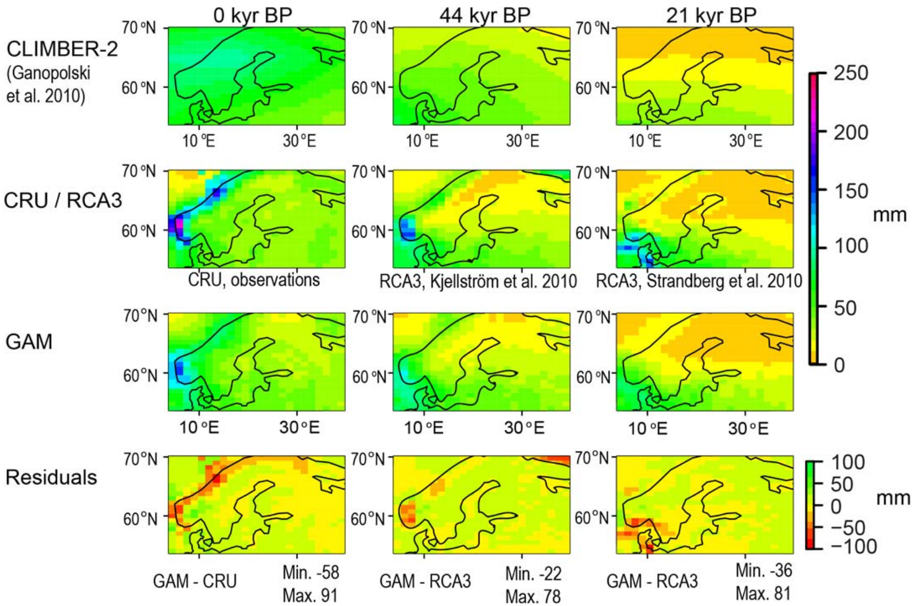

Fig. 3. January mean total precipitation at 0 kyr BP (left column), at 44 kyr BP (middle column) and at 21 kyr BP (right column) as simulated by the global model CLIMBER-2 (top row), as observed during 1961–1990 by CRU (first figure of the second row), as simulated by the regional model RCA3 (second and third figures of the second row), as predicted by the GAM model (third row), and the difference between the statistical model and observation/simulation (bottom row). Unit: mm. The data of the first and the second rows have been bi-linearly interpolated on to a $1.5^{\circ} \times 0.75^{\circ}$ resolution.

CPD
9, 3371–3398, 2013

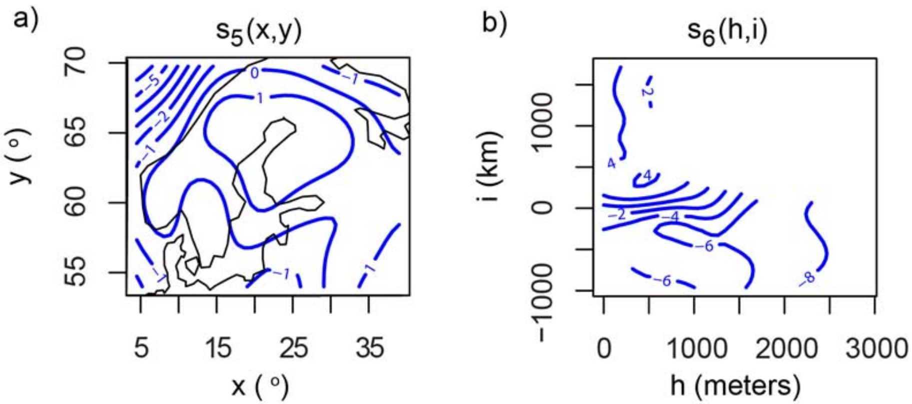

Fig. 4. Components of the GAM model in Eq. (4) fitted to downscale the CLIMBER-2 July mean temperature in the recent past, MIS 3 stadial and LGM climates. The blue curves show the estimated effects of **(a)** longitude and latitude, and **(b)** elevation and distance to the nearest ice sheet (or ice cap) margin. In ice-free areas the distance was expressed by positive values and on areas covered by ice the distance was expressed by negative values.

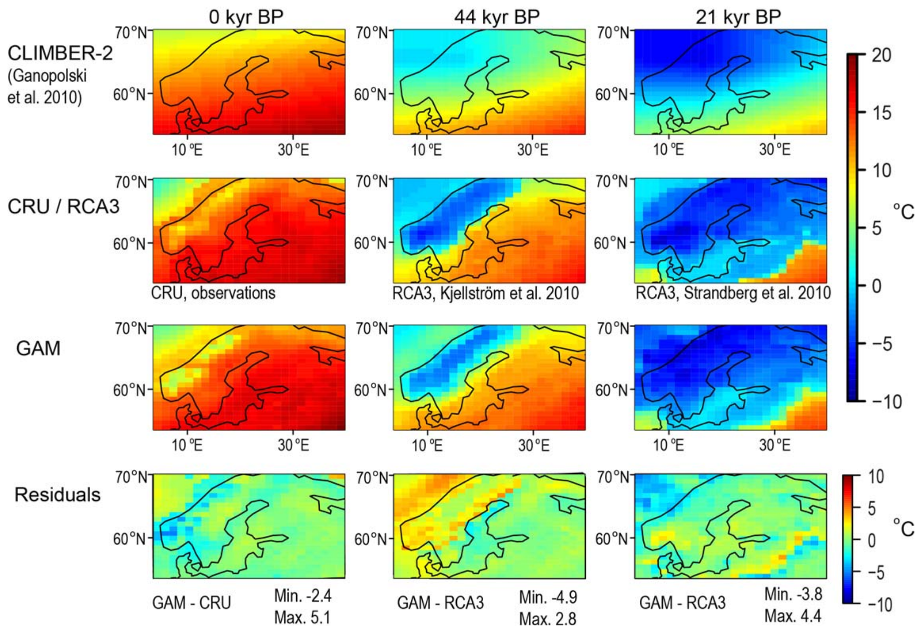

Fig. 5. July mean temperature at 0 kyr BP (left column), at 44 kyr BP (middle column) and at 21 kyr BP (right column) as simulated by the global model CLIMBER-2 (top row), as observed during 1961–1990 by CRU (first figure of the second row), as simulated by the regional model RCA3 (second and third figures of the second row), as predicted by the GAM model (third row), and the difference between the statistical model and observation/simulation (bottom row). Unit: Celsius. The data of the first and the second rows have been bi-linearly interpolated on to a $1.5^{\circ} \times 0.75^{\circ}$ resolution.

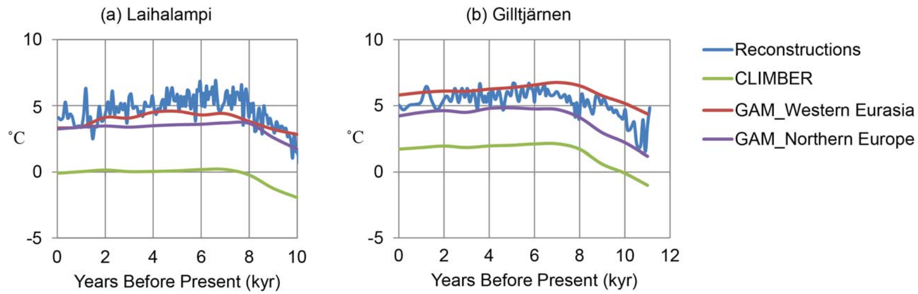

Fig. 6. Comparison of simulation data and pollen-based reconstructions of annual mean temperatures from **(a)** Laihalampi in Finland and **(b)** Gilltjärnen in Sweden. The blue curves represent reconstructions by Heikkilä and Seppä (2003) for Laihalampi, and Antonsson et al. (2006) for Gilltjärnen. The green contours are interpolations from CLIMBER-2 simulations by Ganopolski et al. (2010). The GAM_Western Eurasia (red curves) and GAM_Northern Europe (purple curves) data were downscaled by GAM models from the CLIMBER-2 data in this paper.